

# Effect of Mn-site doping on the magnetotransport properties of the colossal magnetoresistance compound $\text{La}_{2/3}\text{Ca}_{1/3}\text{Mn}_{1-x}\text{A}_x\text{O}_3$ ( $\text{A} = \text{Co}, \text{Cr}$ ; $x \leq 0.1$ )

F. Rivadulla\* and M. A. López-Quintela

*Physical Chemistry Department, University of Santiago de Compostela, E-15706 Santiago de Compostela, Spain*

L. E. Hueso, P. Sande, and J. Rivas

*Applied Physics Department, University of Santiago de Compostela, E-15706 Santiago de Compostela, Spain*

R. D. Sánchez

*Centro Atómico de Bariloche, 8400-San Carlos de Bariloche, Argentina*

(Received 29 February 2000)

In this paper we show the effect of Mn site substitution ( $\leq 10\%$ ) by Co and Cr on the magnetotransport properties of ceramic samples of  $\text{La}_{2/3}\text{Ca}_{1/3}\text{MnO}_3$ . Resistivity, magnetization, and magnetoresistance were systematically investigated as a function of doping. An increase in resistivity and a diminution of metal-insulator transition and Curie temperatures was observed as a consequence of both Co and Cr doping. The evolution of the number of neighbors ferromagnetically coupled to Mn was studied in each sample, and the results suggest some degree of ferromagnetic coupling between  $\text{Cr}^{3+}$  and Mn ions. Implications of both ferromagnetic  $\text{Cr}^{3+}$ -O-Mn $^{3+}$  superexchange and double exchange interactions are discussed. We also found the existence of an optimum doping level that enhances colossal magnetoresistance. This has been explained considering electron localization due to magnetic disorder induced by doping in the Mn site.

## I. INTRODUCTION

The discovery of colossal magnetoresistance (CMR) in mixed valence manganites promoted an extensive number of works about these compounds in the last years.<sup>1,2</sup> Probably one of the most studied is the archetypal  $\text{La}_{2/3}\text{Ca}_{1/3}\text{MnO}_3$ .<sup>3</sup> Schiffer *et al.*<sup>4</sup> obtained the phase diagram of the whole series  $\text{La}_{1-x}\text{Ca}_x\text{MnO}_3$  ( $0 < x < 1$ ) showing a remarkable correlation of magnetic order and electric transport with  $x$ . The simultaneous occurrence of metallicity and ferromagnetism (FM) for intermediate doping levels ( $0.2 \leq x \leq 0.45$ ) has been explained by Zener in the framework of a ferromagnetic double exchange (DE) interaction:<sup>5</sup> the unpaired  $e_g$  electron in the high spin configuration of  $\text{Mn}^{3+}$  moves to a neighboring  $\text{Mn}^{4+}$ , such a transfer being favored if the  $\text{Mn}^{4+}$  which is to receive the electron has its own spins ( $S = 3/2$ ,  $t_{2g}^3$ ) aligned parallel with respect to  $\text{Mn}^{3+}$  spins. In this scenario, electron delocalization between Mn ions leads to a lowering of energy, and will favor a ferromagnetic ordering of the magnetic moments. Several works have shown how DE interaction, and hence FM coupling and CMR, can be tuned by changing the mean ionic radius at the rare-earth site.<sup>6,7</sup> But although this is one of the most studied topics of solid-state physics, not too much is known about the effect of substitution in the Mn site, even though it acts at the heart of DE interaction.

Ahn *et al.*<sup>8</sup> reported the effect of Fe doping on the magnetic and CMR properties of  $\text{La}_{0.63}\text{Ca}_{0.37}\text{MnO}_3$ . In this case, electron hopping between Fe and Mn is impeded by the lack of available states in the Fe  $e_g^\uparrow$  band. Consequently, Fe causes a depletion of the available hopping sites and DE is suppressed. Similar results were found by Blasco *et al.*<sup>9</sup> and by Y. Sun *et al.*<sup>10</sup> when doping  $\text{La}_{0.67}\text{Ca}_{0.33}\text{MnO}_3$  with  $\text{Al}^{3+}$

and  $\text{Ga}^{3+}$ , respectively. J. R. Sun *et al.*<sup>11</sup> reported marked differences for  $\text{Fe}^{3+}$  and  $\text{Ge}^{4+}$  doping in  $\text{La}_{0.7}\text{Ca}_{0.3}\text{MnO}_3$  reflecting different effects due to electron or hole trapping. Ghosh *et al.*<sup>12</sup> doped  $\text{La}_{0.67}\text{Ca}_{0.33}\text{MnO}_3$  with a 5% of the entire first transition element series and found a correlation between the maximum MR, the lattice parameter, and the ionic radii of these elements. Gayathri *et al.*<sup>13</sup> studied the  $\text{La}_{0.7}\text{Ca}_{0.3}\text{Mn}_{1-x}\text{Co}_x\text{O}_3$  series and found that Co substitution suppresses the CMR characteristic of the undoped manganite over the entire temperature and composition range. They argue a transition from a long-range ferromagnetic order to a cluster glass-type ferromagnetism due to Co doping, even for the lowest degree of substitution. Moreover, for  $x > 0.05$  they observed semiconducting behavior in the whole temperature range. However, Rubinstein *et al.*<sup>14</sup> found that up to 20% of Co substitution,  $\text{La}_{2/3}\text{Ca}_{1/3}\text{MnO}_3$  is metallic below the ferro-paramagnetic transition temperature. On the other hand, it has been recently reported that Cr doping in  $\text{Sm}_{0.5}\text{Ca}_{0.5}\text{MnO}_3$  destroys the low-temperature antiferromagnetic-charge ordered state to induce a FM-metallic component in this material.<sup>15</sup> This has been used as a proof of the ability of Cr to be DE coupled with Mn ions. The aim of this paper is to study the effect of a low degree of substitution by two different magnetic ions under controversy (Co and Cr) on the magnetotransport properties of the CMR compound  $\text{La}_{2/3}\text{Ca}_{1/3}\text{MnO}_3$ . As we have checked by x-ray diffraction, no appreciable changes in the lattice structure are produced at these low doping levels, and the effects due to electronic mismatch between Mn and Co/Cr become the only relevant.

## II. EXPERIMENTAL DETAILS

Two series of polycrystalline  $\text{La}_{2/3}\text{Ca}_{1/3}\text{Mn}_{1-x}\text{Co}_x\text{O}_3$  (LCMCo) and  $\text{La}_{2/3}\text{Ca}_{1/3}\text{Mn}_{1-x}\text{Cr}_x\text{O}_3$  (LCMCr) ( $x = 0$ ,

TABLE I. Theoretical and experimental stoichiometry, referred to Ca content, of ceramic samples obtained by x-ray fluorescence spectrometry.

Theoretical	Experimental	% Co, Cr in Mn site
$\text{La}_{0.67}\text{Ca}_{0.33}\text{Mn}$	$\text{La}_{0.6698}\text{Ca}_{0.33}\text{Mn}_{1.017}$	
$\text{La}_{0.67}\text{Ca}_{0.33}\text{Mn}_{0.975}\text{Co}_{0.025}$	$\text{La}_{0.672}\text{Ca}_{0.33}\text{Mn}_{1.03}\text{Co}_{0.0259}$	2.45
$\text{La}_{0.67}\text{Ca}_{0.33}\text{Mn}_{0.95}\text{Co}_{0.05}$	$\text{La}_{0.655}\text{Ca}_{0.33}\text{Mn}_{0.988}\text{Co}_{0.053}$	5.09
$\text{La}_{0.67}\text{Ca}_{0.33}\text{Mn}_{0.925}\text{Co}_{0.075}$	$\text{La}_{0.655}\text{Ca}_{0.33}\text{Mn}_{0.95}\text{Co}_{0.078}$	7.59
$\text{La}_{0.67}\text{Ca}_{0.33}\text{Mn}_{0.9}\text{Co}_{0.1}$	$\text{La}_{0.663}\text{Ca}_{0.33}\text{Mn}_{0.92}\text{Co}_{0.105}$	10.24
$\text{La}_{0.67}\text{Ca}_{0.33}\text{Mn}_{0.975}\text{Cr}_{0.025}$	$\text{La}_{0.65}\text{Ca}_{0.33}\text{Mn}_{1.00}\text{Cr}_{0.024}$	2.34
$\text{La}_{0.67}\text{Ca}_{0.33}\text{Mn}_{0.95}\text{Cr}_{0.05}$	$\text{La}_{0.686}\text{Ca}_{0.33}\text{Mn}_{1.09}\text{Cr}_{0.0735}$	6.79
$\text{La}_{0.67}\text{Ca}_{0.33}\text{Mn}_{0.925}\text{Cr}_{0.075}$	$\text{La}_{0.677}\text{Ca}_{0.33}\text{Mn}_{0.97}\text{Cr}_{0.074}$	7.09
$\text{La}_{0.67}\text{Ca}_{0.33}\text{Mn}_{0.9}\text{Cr}_{0.1}$	$\text{La}_{0.684}\text{Ca}_{0.33}\text{Mn}_{0.95}\text{Cr}_{0.10}$	9.52

0.025, 0.05, 0.075, 0.10) were prepared by standard ceramic procedures. Stoichiometric mixtures of  $\text{La}_2\text{O}_3$ ,  $\text{CaCO}_3$ ,  $\text{Mn}_2\text{O}_3$ ,  $\text{MnO}_2$ , and  $\text{Co}(\text{NO}_3)_2$  or  $\text{Cr}(\text{NO}_3)_3$  (at least 99.99% in purity) were grounded, pressed, and heated in air at 1000 °C for 10 h. After this step, the Co/Cr nitrates has been confirmed to transform into their oxides by x-ray diffraction. After grinding, they were pressed into pellets and sintered in air at 1100 °C for 70 h, 1200 °C for 30 h, and 1300 °C for 100 h with intermediate grindings. Cationic content of these samples was measured by x-ray fluorescence with a Siemens SRS 3000 spectrometer. Samples were melted with  $\text{BO}_4\text{Li}$ ,  $\text{CO}_3\text{Na}_2$ ,  $\text{NO}_3\text{NH}_4$ , and  $\text{LiBr}$  in a Pt crucible at 1100 °C. More than 20 reference patterns with different concentrations of La, Ca, Mn, Cr, and Co were prepared in order to obtain the exact stoichiometry of ceramic samples.

Structural information was derived using the program LS1, based on the Rietveld method, and fitting profiles to pseudo-Voigt functions.<sup>16</sup> Zero-field-cooling (ZFC) ( $M_{\text{ZFC}}$ ) and field-cooling (FC) ( $M_{\text{FC}}$ ) magnetization curves were measured with a vibrating-sample magnetometer between 100 and 300 K at 10 Oe. Under such small applied field, the Curie temperature ( $T_C$ ) can be obtained very accurately from the peak in  $dM_{\text{FC}}/dT$ . The dc magnetic susceptibility  $\chi(T)$  was measured above  $T_C$  up to 1000 K with a Faraday balance at 5 kOe.

### III. EXPERIMENTAL RESULTS

#### A. Structure and chemistry

In Table I we show the comparison between expected and experimentally determined stoichiometry in ceramic samples. Most of them present only slight deviations from the desired composition. In the rest of the paper we will refer to the samples using the experimental composition.

Structural parameters deduced from the Rietveld refinement of the x-ray-diffraction patterns of ceramic samples are summarized in Fig. 1. All the compounds are orthorhombic ( $Pbnm$ ) with the  $\text{O}'$  structure ( $c/\sqrt{2} < a < b$ ). Substitution with Co or Cr does not substantially change the structure of the undoped compound, although slight variations in the unit-cell volume ( $< 0.5\%$ ) are evident due to differences in the ionic radii of Co/Cr and Mn. Sample  $\text{La}_{0.684}\text{Ca}_{0.33}\text{Mn}_{0.95}\text{Cr}_{0.10}\text{O}_{3\pm\delta}$  does not follow the gradual reduction of volume observed in the series. This sample was

also synthesized under an  $\text{O}_2$  current in order to prevent for possible oxygen vacancies, but the results were practically identical to the sample made under air atmosphere. In any case, the volume variation with respect to the  $x=0$  sample is lower than 0.5%.

#### B. Magnetotransport properties

Figure 2 shows the temperature dependence of resistivity (left panel) and magnetization (right panel) of LCMCo (top) and LCMCr (bottom). Higher doping level results in lower metal-insulator transition temperatures ( $T_{MI}$ ) and higher residual and peak resistivities. On the other hand, above  $T_{MI}$  all the samples follow a universal curve characteristic of a thermally assisted conduction mechanism. The Curie temperature (Fig. 3) also reduces with doping, following  $T_{MI}$ .

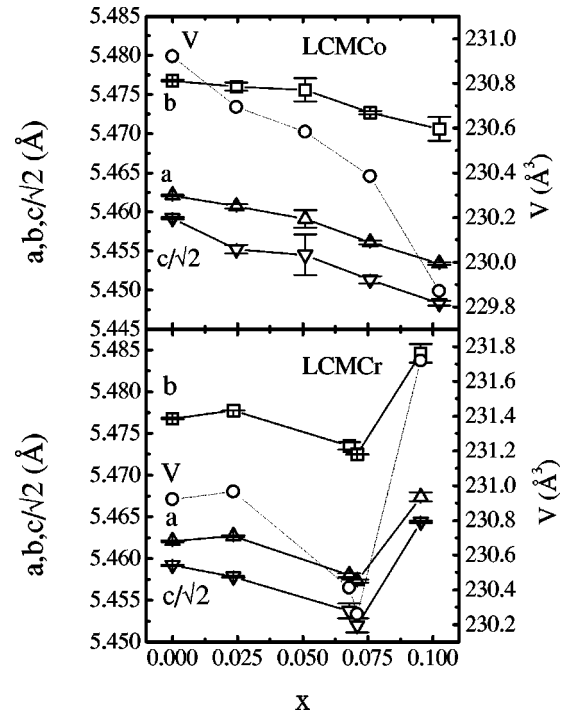


FIG. 1. Evolution of volume and lattice parameters with Co (top) and Cr (bottom) concentration extracted from Rietveld refinement of x-ray powder data of ceramic samples. For the adjustment we have used site occupancies obtained from x-ray fluorescence analysis.

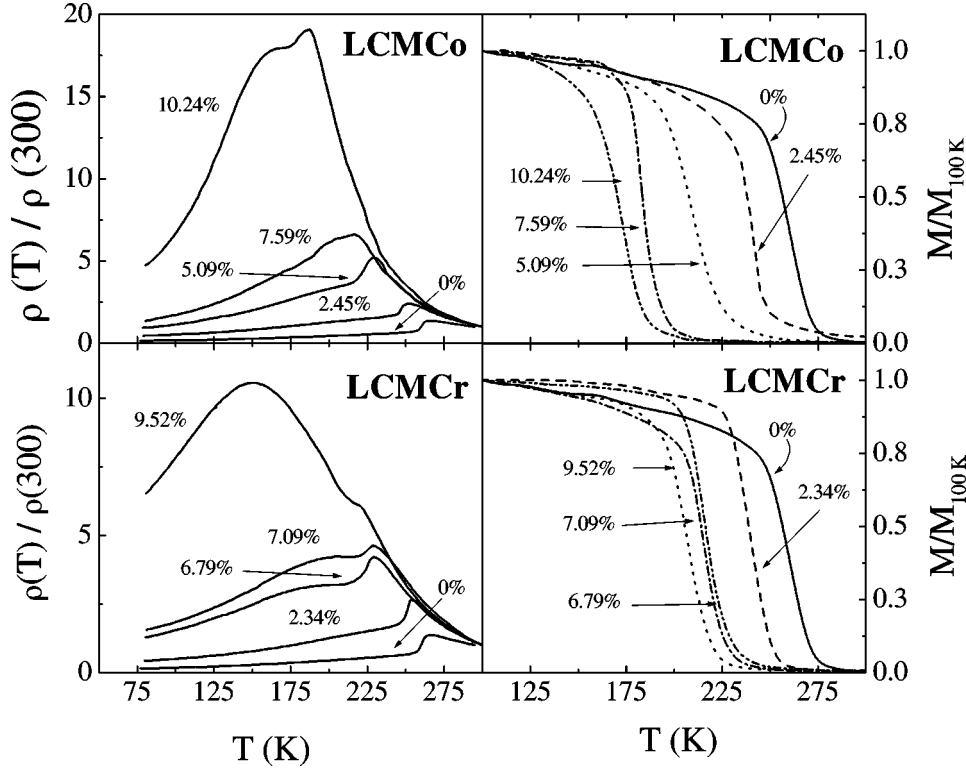


FIG. 2. Temperature dependence of resistivity (left panel) and magnetization (right panel) of LCMCo (top) and LCMCr (bottom) series.

However, the linear reduction of  $T_C$  produced by Co is not observed in Cr series, where a tendency to stabilization at about 210 K is clearly observed. Anyway,  $T_C$  is always smaller than  $T_{MI}$ , except in  $\text{La}_{0.684}\text{Ca}_{0.33}\text{Mn}_{0.95}\text{Cr}_{0.10}\text{O}_{3\pm\delta}$ . This could be the signature of the presence of a high degree of oxygen vacancies in this sample.

Between  $T_C$  and  $T_{MI}$ , samples are in a mixed state of paramagnetic (PM) and ferromagnetic phases.<sup>17</sup> The presence of a short-range FM order between  $T_C$  and  $T_{MI}$  produces a charge localization and an abrupt rise of resistivity, but the sample remains metalliclike ( $d\rho/dT > 0$ ) if transport time is comparable to the lifetime of these short range FM correlations and some degree of delocalization persist.

In Fig. 4(a) we show the magnetoresistance isotherms ( $T = T_{MI}$ ) measured up to 7.5 kOe for some samples as a function of doping. In both series, LCMCo (top) and LCMCr

(bottom) we observed a systematic increase of the % CMR up to  $\sim 5\%$  of doping. For higher doping % CMR decreases again [Fig. 4(b)]. This reflects the existence of an optimum doping level that favors CMR, whatever the nature of the dopant. It should be noted that we have doubled the value of the intrinsic magnetoresistance of  $\text{La}_{2/3}\text{Ca}_{1/3}\text{MnO}_3$  associated to the FM-PM transition with only  $\sim 5\%$  of Co doping. In Fig. 5  $M_{FC-ZFC}$  curves, representative of the general behavior of the two series of samples are presented. For  $x \geq 0.05$ , a strong dependence of  $M_{ZFC}$  curves below  $T_C$  becomes evident in Co samples. This effect is not observed in Cr samples, where a temperature-independent behavior of the  $M_{ZFC}$ , similar to the  $x=0$  sample, is observed in all the series. The drop of the  $M_{ZFC}$  curve for  $x \geq 0.05$  is an indication of the absence of long-range FM order and is a signature of cluster-glass-like behavior in highly doped Co samples. On the other hand, the almost temperature-independent  $M_{ZFC}$  curves of Cr samples below  $T_C$  is a signature of a well established long-range FM order.

High-temperature magnetic susceptibility [ $\chi(T)$ ] follows a Curie-Weiss law. Below  $\approx 1.4\Theta$  (where  $\Theta$  is the paramagnetic Curie-Weiss temperature)  $\chi^{-1}(T)$  shows a positive curvature and  $T_C < \Theta$ . From the linear part of the plot  $\chi^{-1}(T)$  we have derived the Curie constant ( $C$ ) and  $\Theta$  for each sample (see Table II).

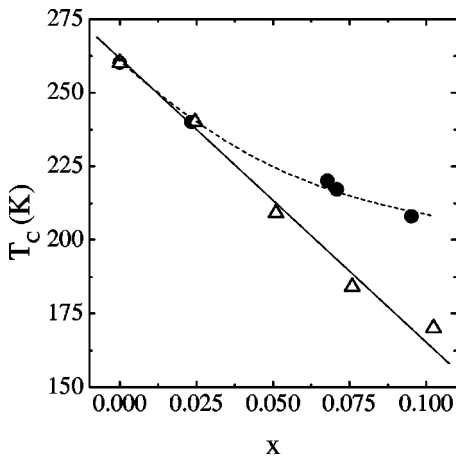


FIG. 3. Dependence of  $T_C$  with % Co ( $\Delta$ ) and % Cr ( $\bullet$ ). Lines are guides to the eye.

#### IV. DATA ANALYSIS AND DISCUSSION

The observed reduction of  $T_{MI}$  and  $T_C$  (Figs. 2 and 3) cannot be described by a variation in the  $\text{Mn}^{3+}/\text{Mn}^{4+}$  relationship, as the phase diagram for  $\text{La}_{0.67}\text{Ca}_{0.33}\text{MnO}_3$  does not justify the large temperature shifts observed for the low dop-

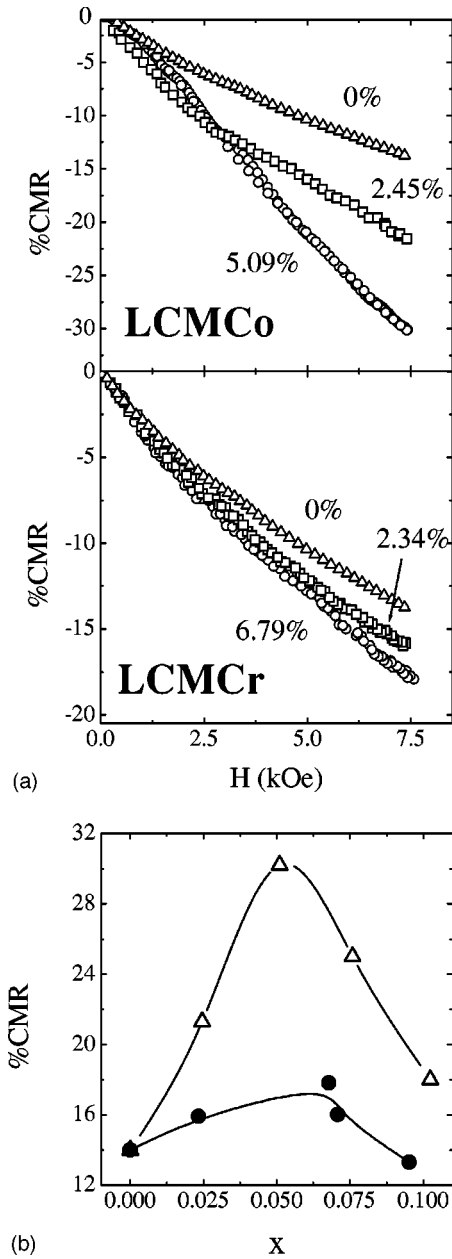


FIG. 4. (a) % CMR vs  $H$  measured at the metal-insulator transition temperature of each sample. (b) CMR at 7.5 kOe for LCMCo ( $\Delta$ ) and LCMCr ( $\bullet$ ).

ing levels discussed here.<sup>4</sup> On the other hand, doping does not substantially affect to the paramagnetic resistivity. At high temperatures, multiphonon-assisted hopping of small polarons occurs between sites through a thermally activated process. Transport measurements by Jaime *et al.*<sup>18</sup> demonstrated that the conductivity in the PM regime of mixed valence manganites is dominated by the thermally activated hopping of small polarons in the adiabatic limit. We have obtained values for the polaron hopping energy  $E_p \approx 175 \pm 15$  meV, irrespective of dopant and doping level. De Teresa *et al.*<sup>19</sup> found that small variations in the  $\text{Mn}^{3+}$  content of CMR manganites have extraordinary effects in the polaron hopping energy, evidencing the Jahn-Teller (JT) nature of these polarons. The almost constant value of  $E_p$  is an indication of the practical invariance in the  $\text{Mn}^{3+}/\text{Mn}^{4+}$  ratio in our samples. Very recently, Gosh *et al.*<sup>12</sup> reported the

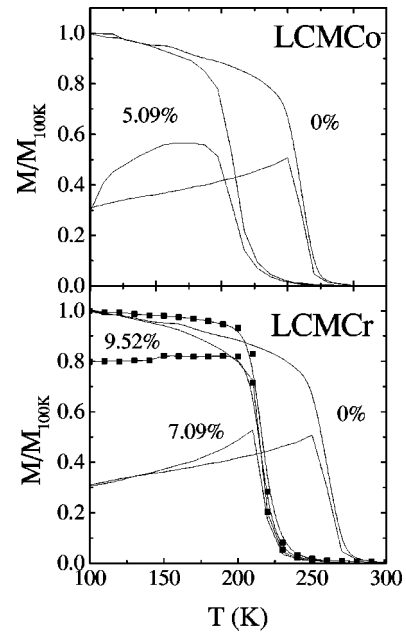


FIG. 5. FC-ZFC curves representative of the general behavior in both series. Doping levels  $x \geq 0.05$  produces the observed temperature dependence of the ZFC curve below  $T_C$  in Co samples (top). This is not observed in Cr series (bottom).

effect of ionic radii mismatch at the Mn site for all the elements of the first transition series at a fixed dopant concentration (5%) in  $\text{La}_{0.7}\text{Ca}_{0.3}\text{MnO}_3$ . They attribute a central role to lattice strains in controlling the magnetotransport of the system. However, a variation of  $\sim 20$  K for  $x \approx 0.025$  cannot be justified in the basis of their results. Moreover, the enhancement of % CMR (measured at  $T_{MI}$ ) with doping (Fig. 4) is in contradiction with the strain-CMR correlation proposed in Ref. 12 since slightly lower % CMR should be expected for 5% of Co and Cr substitution.

Since the  $\text{Mn}^{3+}/\text{Mn}^{4+}$  ratio is approximately constant for all the samples, the variations in  $\Theta$  reflect the changes in the isotropic exchange interactions, and the degree of magnetic frustration induced with doping can be measured through the ratio  $T_C/\Theta$ . For  $x=0$ ,  $T_C/\Theta \approx 0.71$ , close to the value of 0.78 predicted by the constant coupling approximation (CCA).<sup>20</sup> This ratio tends to decrease with doping (see Table II) but is more dramatic for Co than for Cr samples. This result suggests that the magnetic frustration induced by Co

TABLE II. Values for the Curie constant, Curie-Weiss, and Curie temperatures obtained from susceptibility measurements.

Compound	$C$ (emu K/mol)	$\theta$ (K)	$T_C$ (K)	$T_C/\theta$
$\text{La}_{0.6698}\text{Ca}_{0.33}\text{Mn}_{1.017}\text{O}_{3 \pm \delta}$	2.8(1)	368	260	0.706
LCMCo 2.45%	2.7(1)	343	240	0.7
5.09%	2.5(1)	392	209	0.53
7.59%	2.7(2)	353	184	0.52
10.24%	2.6(1)	371	170	0.43
LCMCr 2.34%	2.7(1)	383	240	0.627
6.79%	2.6(2)	342	220	0.643
7.09%	2.6(1)	332	217	0.654
9.52%	2.6(3)	339	208	0.614



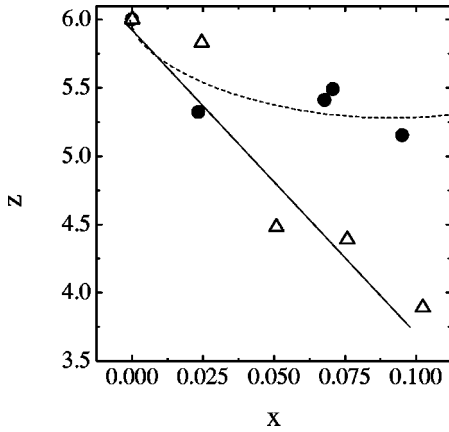


FIG. 6. Evolution of the effective number of neighbors ferromagnetically coupled to Mn as a function of doping in LCMCo ( $\Delta$ ) and LCMCr ( $\bullet$ ). Lines are guides to the eye.

doping in the Mn sublattice is larger than induced by Cr. Within the CCA, the effective number of neighbors FM coupled to Mn can be derived from the values of  $T_C/\Theta$ . Results are plotted in Fig. 6. While Co produces a reduction approximately linear of the number of neighbors with doping, Cr only reduces the neighbors in a small quantity and tends to a stable value of about 5.25. From this result it follows that Co does not participate in DE interaction, but there is some degree of FM coupling between Cr and Mn ions. The electronic configuration of Co is very complicated due to the existence of several possible spin states. Apart from low and high spin, Bahadur *et al.*<sup>21</sup> reported ferromagnetic resonance data supporting the existence of intermediate spin configurations for  $\text{Co}^{3+}$  ( $t_{2g}^5 e_g^1$ ) and  $\text{Co}^{4+}$  ( $t_{2g}^4 e_g^1$ ) in mixed-valence cobaltites. Moreover, the possibility of temperature induced transitions from low to localized-intermediate and to delocalized-intermediate spin states has been demonstrated in the parent compound  $\text{LaCoO}_3$ .<sup>22</sup> On the other hand,  $\text{Cr}^{3+}$  ( $t_{2g}^3 e_g^0$ ) is the only ion replacing manganese in the LCMCr series. In the view of these electronic configurations, it seems reasonable to think in  $\text{Cr}^{3+}$  as the only possible candidate to establish a FM interaction with Mn ions.  $\text{Cr}^{3+}$  is isoelectronic with  $\text{Mn}^{4+}$  and DE interaction should be possible between  $\text{Mn}^{3+}$  and  $\text{Cr}^{3+}$ , although the different effect of the crystal field over  $\text{Mn}^{4+}$  and  $\text{Cr}^{3+}$  must cause energetic differences between  $e_g^\uparrow$  levels of  $\text{Mn}^{3+}$  and  $\text{Cr}^{3+}$  strong enough to make electronic exchange between them not so effective as between  $\text{Mn}^{3+}$  and  $\text{Mn}^{4+}$ . Moreover,  $\text{Cr}^{3+}$  ions take their positions presumably at random at the time of sample preparation, whereas only electron transfer is necessary to produce ordering of  $\text{Mn}^{3+}$  and  $\text{Mn}^{4+}$  ions. On the other hand,  $\text{Cr}^{3+}$ -O- $\text{Mn}^{3+}$  superexchange interaction is ferromagnetic, and should be taken into account in order to explain our results.<sup>23</sup> This interaction leads to FM allignment of  $\text{Cr}^{3+}$  and  $\text{Mn}^{3+}$  keeping the number of neighbors FM coupled to Mn near to 6. In a neutron-diffraction study of the magnetic structure of  $\text{La}(\text{Mn,Cr})\text{O}_3$ , Bents<sup>24</sup> showed that a low percentage of  $\text{Cr}^{3+}$  destroys the A-type AF structure of  $\text{LaMnO}_3$ , and produces the spin reversal of some of its nearest  $\text{Mn}^{3+}$  neighbors via superexchange coupling leading to a FM moment. The rate of destruction of the AF phase by  $\text{Cr}^{3+}$ -O- $\text{Mn}^{3+}$  FM superexchange is compa-

rable to that observed when  $\text{Mn}^{3+}$  is replaced by  $\text{Mn}^{4+}$  and FM DE interaction is established.

Very recently, a number of experimental works built up the idea of the participation of  $\text{Cr}^{3+}$  in DE. In example, paramagnetic-insulating to ferromagnetic-metallic transitions were induced in  $\text{Sm}_{0.5}\text{Ca}_{0.5}\text{MnO}_3$  by Cr doping ( $0.05 \leq x \leq 0.09$ ).<sup>15</sup> Raveau *et al.*<sup>25</sup> find that Cr, Co, and Ni kills the charge ordering state in  $\text{Pr}_{0.5}\text{Ca}_{0.5}\text{MnO}_3$  restoring a metal-insulator transition high values of magnetization. However, the maximum value of the magnetic moment is larger for Cr doped samples, and the doping effect is extended for a largest range of Cr substitution (3–10%). As a result of this doping effect, participation of Cr in de DE mechanism has been proposed. However, Damay *et al.*<sup>26</sup> reported an induced antiferromagnetic-insulating to ferromagnetic-metallic transition in the charge ordered (CO) compound  $\text{Pr}_{0.6}\text{Ca}_{0.4}\text{MnO}_3$  by doping with  $\text{Fe}^{3+}$  ( $3d^5$ ),  $\text{Al}^{3+}$  ( $3d^0$ ),  $\text{Ga}^{3+}$  ( $3d^0$ ), and  $\text{Mg}^{2+}$  ( $3s^0$ ). A strong FM component ( $2.1\mu_B$  for  $x = 0.035$ ) is induced by iron doping. Since these ions cannot establish an effective DE interaction with Mn due to their electronic configuration, it easily follows that the weakening of the CO-AF ground state by Mn site doping in CO manganites is developed by the introduction of some degree of disorder in the Mn sublattice. On the other hand, the increasing magnetic moment induced by Cr doping can be successfully explained considering FM superexchange interaction only. The presence of this interaction also justify why this doping induced FM component is restricted to a small percentage of substitution. For higher percentages of  $\text{Cr}^{3+}$ , formation of  $\text{Cr}^{3+}$ -O- $\text{Cr}^{3+}$  and  $\text{Cr}^{3+}$ -O- $\text{Mn}^{4+}$  pairs become more favorable, leading to growing AF superexchange interactions.

So, we believe that participation of Cr in the DE interaction cannot be deduced from these results, and the behavior observed in CO manganites cannot be extrapolated to other members of the series, like  $\text{La}_{2/3}\text{Ca}_{1/3}\text{MnO}_3$ . Although in this work we clearly show the existence of FM coupling between  $\text{Mn}^{3+}$  and  $\text{Cr}^{3+}$  in  $\text{La}_{2/3}\text{Ca}_{1/3}\text{MnO}_3$ , we cannot ensure that  $\text{Cr}^{3+}$  participates in the DE, as we believe that the possibility of FM superexchange interaction must been taken into account in order to explain these results.

We showed how Co makes the Mn sublattice more disordered that Cr, from a magnetic point of view. This magnetic disorder leads to a localization of conduction electrons, in a similar way as it was pointed out by Anderson (Anderson localization).<sup>27</sup> In the Anderson model a mobility edge  $E_b$  can be defined to separate localized states of the tail band from extended states of the middle of the band. Metal-insulator transition occurs when the Fermi level ( $E_F$ ) moves, through the mobility edge, from a extended state to a localized state. The increasing residual resistivity and decreasing  $T_{MI}$  observed with doping in our samples is a consequence of increasing disorder. Moreover, replacement of Mn by Co or Cr leads to some degree of magnetic disorder superimposed to the nonmagnetic one (see Fig. 6). Doping produces an effect very similar to the effect of temperature, i.e.,  $E_b$  grows and becomes larger than  $E_F$ , which now is a localized state. As CMR isotherms of Fig. 4(a) are measured at the corresponding  $T_{MI}$ , the effective temperature is the same for each sample. The effect of the applied field is to alter the localization length, reducing  $E_b$ , being  $E_F$  in the middle of

the extended states. For doping levels larger than  $\sim 5\%$ ,  $E_b \gg E_F$  and the effect of 7.5 kOe is not so strong as to make  $E_b < E_F$ .

Sheng *et al.*<sup>28</sup> argued that the presence of a certain quantity of randomness, along with the effective hopping disorder of the DE model, produces an Anderson metal-to-insulator transition associated to the FM-PM transition. These authors proposed the existence of an optimum value of nonmagnetic disorder strength that favors the CMR effect. Our data fully support their theoretical predictions, although the type of disorder here introduced is not exactly the same referred by Sheng.

As we have mentioned, nonintrinsic effects appear for  $x \geq 0.05$  in Co samples. The number of DE-inactive species introduced by Co doping at the Mn site, is high enough to break the long-range magnetic coherence when  $x \geq 0.05$ . Ritter *et al.*<sup>29</sup> proposed that  $\sim 5\%$  of Mn site vacancies are responsible for the appearance of a cluster-glass state in  $\text{La}_{3/(3+\delta)}\text{Mn}_{3/(3+\delta)}\text{O}_3$  (%  $\text{Mn}^{4+} = 2\delta \times 100$ ). The assumption of the presence of high magnetic disorder above  $x \approx 0.05$  in Co samples is supported by the behavior of the  $M_{FC-ZFC}$  curves as a function of doping (Fig. 5).  $M_{ZFC}$  for  $x < 0.05$  are almost independent of  $T$  below  $T_C$  as in the pure manganite ( $x = 0$ ). This is a signature of a well established long-range FM order. However, for  $x \geq 0.05$  a strong dependence of  $M_{ZFC}$  curves below  $T_C$  becomes evident in Co series. The drop of the  $M_{ZFC}$  curve for % Co = 5.09 is an indication of the absence of long-range FM order and is a signature of cluster-glass-like behavior. From these results we conclude that the most likely state in our highly doped Co samples is formed by FM clusters in a background with ferro-antiferromagnetic competing interactions, which probably lead to an overall cluster glass behavior.

## V. CONCLUSIONS

We have tested the effect of Co and Cr doping on the magnetotransport behavior of the CMR compound  $\text{La}_{2/3}\text{Ca}_{1/3}\text{MnO}_3$ . We have found that Cr doping only produces a slight reduction in the number of neighbors ferromagnetically coupled to Mn, while Co dramatically reduces it. From these results it follows that  $\text{Cr}^{3+}$  is able to be FM coupled with  $\text{Mn}^{3+}$  but success was achieved in accounting for these data on the basis of a FM  $\text{Cr}^{3+}$ -O- $\text{Mn}^{3+}$  superexchange. It is then concluded that participation of  $\text{Cr}^{3+}$  in DE mechanism cannot be deduced from these experimental results. Moreover, our results show that both structural and magnetic disorder induced in the periodic lattice potential at low doping levels can be exploited to enhance the intrinsic CMR of the system, in perfect accordance with theoretical predictions. Mn-site doping of CMR compounds with  $T_C$  over room temperature could be used to achieve higher magnetoresistance values at room temperature.

## ACKNOWLEDGMENTS

We want to express our gratitude to Dr. M. T. Causa from the Centro Atómico de Bariloche (Argentina) for her helpful discussion of the results and critical reading of the manuscript, Jorge Millos from the University of Vigo (Spain) for compositional analysis of ceramic samples, and to M. Vázquez-Mansilla, from the Centro Atómico de Bariloche for measurements with the Faraday balance. Two of us (F.R. and L.E.H.) want to acknowledge support from USC and MEC of Spain. We also thank MEC from Spain for financial support through Project No. MAT98-0416.

\*Corresponding author. Email address: qffran@usc.es

<sup>1</sup>R. von Helmolt, J. Wecker, B. Holzapfel, L. Schultz, and K. Samwer, Phys. Rev. Lett. **71**, 2331 (1993).

<sup>2</sup>S. Jin, T. H. Tiefel, M. McCormack, R. A. Fastnacht, R. Ramesh, and L. H. Chen, Science **264**, 413 (1994).

<sup>3</sup>G. H. Jonker and J. H. van Santen, Physica (Amsterdam) **16**, 337 (1950).

<sup>4</sup>P. Schiffer, A. P. Ramirez, W. Bao, and S. W. Cheong, Phys. Rev. Lett. **75**, 3336 (1995).

<sup>5</sup>C. Zener, Phys. Rev. **82**, 403 (1951).

<sup>6</sup>H. Y. Hwang, S.-W. Cheong, P. G. Radaelli, M. Marezio, and B. Batlogg, Phys. Rev. Lett. **75**, 914 (1995).

<sup>7</sup>J. Fontcuberta, B. Martinez, A. Seffar, S. Piñol, J. L. Garcia-Muñoz, and X. Obradors, Phys. Rev. Lett. **76**, 1122 (1996).

<sup>8</sup>K. H. Ahn, X. W. Wu, K. Liu, and C. L. Chien, Phys. Rev. B **54**, 15 299 (1996).

<sup>9</sup>J. Blasco, J. García, J. M. de Teresa, M. R. Ibarra, J. Pérez, P. A. Algarabel, C. Marquina, and C. Ritter, Phys. Rev. B **55**, 8905 (1997).

<sup>10</sup>Y. Sun, X. Xu, L. Zheng, and Y. Zhang, Phys. Rev. B **60**, 12 317 (1999).

<sup>11</sup>J. R. Sun, G. H. Rao, B. G. Shen, and H. K. Wong, Appl. Phys. Lett. **73**, 2998 (1998).

<sup>12</sup>K. Gosh, S. B. Ogale, R. Ramesh, R. L. Greene, T. Venkatesan, K. M. Gapchup, R. Bathe, and S. I. Patil, Phys. Rev. B **59**, 533 (1999).

<sup>13</sup>N. Gayathri, A. K. Raychaudhuri, S. Tiwary, R. Gundakaram, A. Arulraj, and C. N. R. Rao, Phys. Rev. B **56**, 1345 (1997).

<sup>14</sup>M. Rubinstein, D. J. Gillespie, J. E. Snyder, and T. M. Tritt, Phys. Rev. B **56**, 5412 (1997).

<sup>15</sup>A. Barnabé, A. Maignan, M. Hervieu, F. Damay, C. Martin, and B. Raveau, Appl. Phys. Lett. **71**, 3907 (1997).

<sup>16</sup>L. Lutterotti, P. Scardi, and P. Maistrelli, J. Appl. Crystallogr. **25**, 459 (1992); see also, for example, *The Rietveld Method*, edited by R. A. Young, IUCr-Monographs on Crystallography, Vol. 5 (Oxford University Press, New York, 1995), Chap. 8.

<sup>17</sup>Z. W. Lin, J. W. Cochrane, G. J. Russell, X. L. Wang, S. X. Dou, and H. K. Liu, Appl. Phys. Lett. **74**, 3014 (1999).

<sup>18</sup>M. Jaime, H. T. Hardner, M. B. Salomon, M. Rubinstein, P. Dorsey, and D. Emin, Phys. Rev. Lett. **78**, 951 (1997).

<sup>19</sup>J. M. De Teresa, K. Dorr, K. H. Müller, L. Schultz, and R. I. Chakalova, Phys. Rev. B **58**, 5928 (1998).

<sup>20</sup>J. S. Smart, in *Effective Field Theories of Magnetism* (W. B. Saunders Company, Philadelphia & London, 1966), Chap. V; M. T. Causa, M. Tovar, A. Caneiro, F. Prado; G. Ibanez, C. A. Ramos, A. Butera, B. Alascio, X. Obradors, S. Pinol, F. Rivadulla, C. Vazquez-Vazquez, M. A. Lopez-Quintela, J. Rivas, Y. Tokura, and S. B. Oseroff, Phys. Rev. B **58**, 3233 (1998).

<sup>21</sup>D. Bahadur, S. Kollali, C. N. R. Rao, M. J. Patni, and C. M. Srivastava, J. Phys. Chem. Solids **40**, 981 (1979).

<sup>22</sup>M. A. Señaris-Rodríguez and J. B. Goodenough, J. Solid State Chem. **116**, 224 (1995).

- <sup>23</sup>J. B. Goodenough and J. M. Longo, in *Magnetic and Other Properties of Oxides and Related Compounds*, edited by K.-H. Hellwege and A. M. Hellwege, Landolt-Börnstein, New Series, Group III, Vol. 4, Pt. a (Springer, Berlin, 1970).
- <sup>24</sup>U. H. Bents, Phys. Rev. **106**, 225 (1957).
- <sup>25</sup>B. Raveau, A. Maignan, C. Martin, and M. Hervieu, in *Colossal Magnetoresistance, Charge Ordering and Related Properties of Manganese Oxides*, edited by C. N. R. Rao and B. Raveau (World Scientific, Singapore, 1998), Chap. II.
- <sup>26</sup>F. Damay, A. Maignan, C. Martin, and B. Raveau, J. Appl. Phys. **82**, 1485 (1997).
- <sup>27</sup>S. Elliot, in *The Physics and Chemistry of Solids* (John Wiley & Sons, Chichester, UK, 1998), Chap. VI.
- <sup>28</sup>L. Sheng, D. y. Xing, D. N. Sheng, and C. S. Ting, Phys. Rev. Lett. **79**, 1710 (1997).
- <sup>29</sup>C. Ritter, M. R. Ibarra, J. M. De Teresa, P. A. Algarabel, C. Marquina, J. Blasco, J. Garcia, S. Oseroff, and S. W. Cheong, Phys. Rev. B **56**, 8902 (1997).